

Rapid Commun. Mass Spectrom. 2012, 26, 263–268
(wileyonlinelibrary.com) DOI: 10.1002/rcm.5314

Resolution of isomeric multi-ruthenated porphyrins by travelling wave ion mobility mass spectrometry

Priscila M. Lalli¹, Bernardo A. Iglesias², Daiana K. Deda², Henrique E. Toma²,
Gilberto F. de Sa³, Romeu J. Daroda³, Koiti Araki^{2**} and Marcos N. Eberlin^{1*}

¹ThoMSon Mass Spectrometry Laboratory, Institute of Chemistry, University of Campinas, UNICAMP 13083-970, Campinas, SP, Brazil

²University of São Paulo, Institute of Chemistry, Av. Prof. Lineu Prestes 748, CEP 05508-000, São Paulo, SP, Brazil

³National Institute of Metrology, INMETRO, Division of Chemical Metrology 25250-020, Duque de Caxias, RJ, Brazil

The ability of travelling wave ion mobility mass spectrometry (TWIM-MS) to resolve cationic *meta/para* and *cis/trans* isomers of *mono-, di-, tri-* and *tetra-*ruthenated supramolecular porphyrins was investigated. All *meta* isomers were found to be more compact than the *para* isomers and therefore mixtures of all isomeric pairs could be properly resolved with baseline or close to baseline peak-to-peak resolution (R_{p-p}). Di-substituted *cis/trans* isomers were found, however, to present very similar drift times and could not be resolved. N₂ and CO₂ were tested as the drift gas, and similar α but considerably better values of R_p and R_{p-p} were always observed for CO₂. Copyright © 2012 John Wiley & Sons, Ltd.

Porphyrins form a very important class of 18 π -electron conjugated macrocycles exhibiting unique catalytic/electrocatalytic, photochemical and photophysical properties. They are also of great importance in many fields such as biology, medicine, supramolecular chemistry and material and nanomaterial sciences.^[1,2] To generate building blocks for supramolecular assembly, several functional groups have been appended to the *meso-* or β -pyrrole positions of the porphyrin macrocycle so as to promote electrostatic, hydrogen bonding, π - π or hydrophobic intermolecular interactions. The coordination of suitable transition metal complexes is another effective strategy to obtain supramolecular porphyrin systems encompassing redox and/or photochemically active peripheral groups.^[3]

Pyridyl groups are particularly suitable as porphyrin substituents owing to their effective coordination properties.^[4] A series of porphyrin photosensitizers containing transition metal complexes or methyl groups attached to the peripheral pyridyl N-atoms has been therefore envisaged. The interaction of porphyrins with biomolecules can also be finely tuned by playing with isomeric groups imparting different molecular topology and 3D structures to the porphyrin core, such as in the *meso*-substituted *para* and *meta*-pyridylporphyrins. Cationic porphyrins have long been of interest because they can bind to DNA^[5,6] causing damages owing to their photophysical properties, for example acting as potential photosensitizers for

photodynamic inactivation of viruses.^[7] Engelmann *et al.*^[8] have synthesized, characterized and studied the photochemical properties of a series of supermolecular porphyrins, obtained by the coordination of [Ru(bpy)₂Cl]⁺ to the periphery of *meso*-phenyl(pyridyl)porphyrins.

Electrospray ionization mass spectrometry (ESI-MS)^[9] has been established as the gold-standard technique for the characterization of thermally labile and/or polar or ionic organometallic species, such as for many porphyrinic systems.^[10] However, being based primarily on the measurement of m/z ratios, single-stage ESI-MS is inherently unable to distinguish isomers. Strategies based on the correlation between structure and dissociation chemistry via tandem ESI-MS/MS experiments have been therefore used to recognize gaseous isomeric ions.^[10,11] A previous study has characterized a series of cationic macrocyclic complexes formed by the coordination of [Ru(bpy)₂Cl]⁺ to the pyridyl N-atoms of *meso*-(phenyl)_{*m*}-(*meta* or *para*-pyridyl)_{*n*}-porphyrins ($m + n = 4$) by ESI-MS and ESI-MS/MS.^[10] Via ESI-MS/MS, however, the *meta/para* porphyrin isomers could not be distinguished since they promptly dissociate by a sequential 'charge splitting' process that forms [Ru(bpy)₂Cl]⁺ and the complementary cationic fragment thus yielding very similar spectra.

A new dimension for ion analysis has been added to MS, however, via its coupling with ion mobility spectrometry (IMS), where the separation of isomers occurs while the ions migrate through a buffer gas. The drift velocity of an ion depend not only on its mass and charge, but also on its shape (collision cross-section) and polarity,^[12] hence IMS has the potential ability to resolve gaseous isomeric ions. IMS is used mainly to detect drugs, chemical warfare agents, explosives and environmental pollutants,^[13] but its great potential to investigate the conformation of gaseous proteins and peptides has also been demonstrated.^[14] Since then, IMS-MS has also been applied to resolve mixtures of isomeric oligosaccharides and to characterize complex mixtures such

* Correspondence to: M. N. Eberlin, ThoMSon Mass Spectrometry Laboratory, Institute of Chemistry, University of Campinas, UNICAMP 13083-970, Campinas, SP, Brazil.
E-mail: eberlin@iqm.unicamp.br

** Correspondence to: K. Araki, University of Sao Paulo, Institute of Chemistry, Av. Prof. Lineu Prestes 748, CEP 05508-000, São Paulo, SP, Brazil.
E-mail: koiaraki@iq.usp.br

as polymers and crude oils.^[15] In an outstanding example, Hill Jr. *et al.*^[16] used nitrogen doped with 10% (*S*)-(+)-2-butanol in an IMS cell to resolve atenolol enantiomers by IMS-MS.

Travelling wave ion mobility (TWIM) has been introduced as a new mode of ion propulsion for IMS experiments.^[17] In contrast to conventional IMS in which a low electrical field is applied continuously to the IM cell, in TWIM the ions are drifted via the action of a continuous train of transient voltage pulses (travelling waves) applied to pairs of stacked ring electrodes. In total, 122 ring electrodes are encompassed in a very compact (18.5 cm long) ion mobility cell. The ions of lower mobility are overtaken by the waves more often than ions of higher mobility and, consequently, they slip behind the waves and emerge with longer drift times. TWIM cells have been shown to have high transmission efficiency and a separative power comparable with conventional drift cell approaches.^[17]

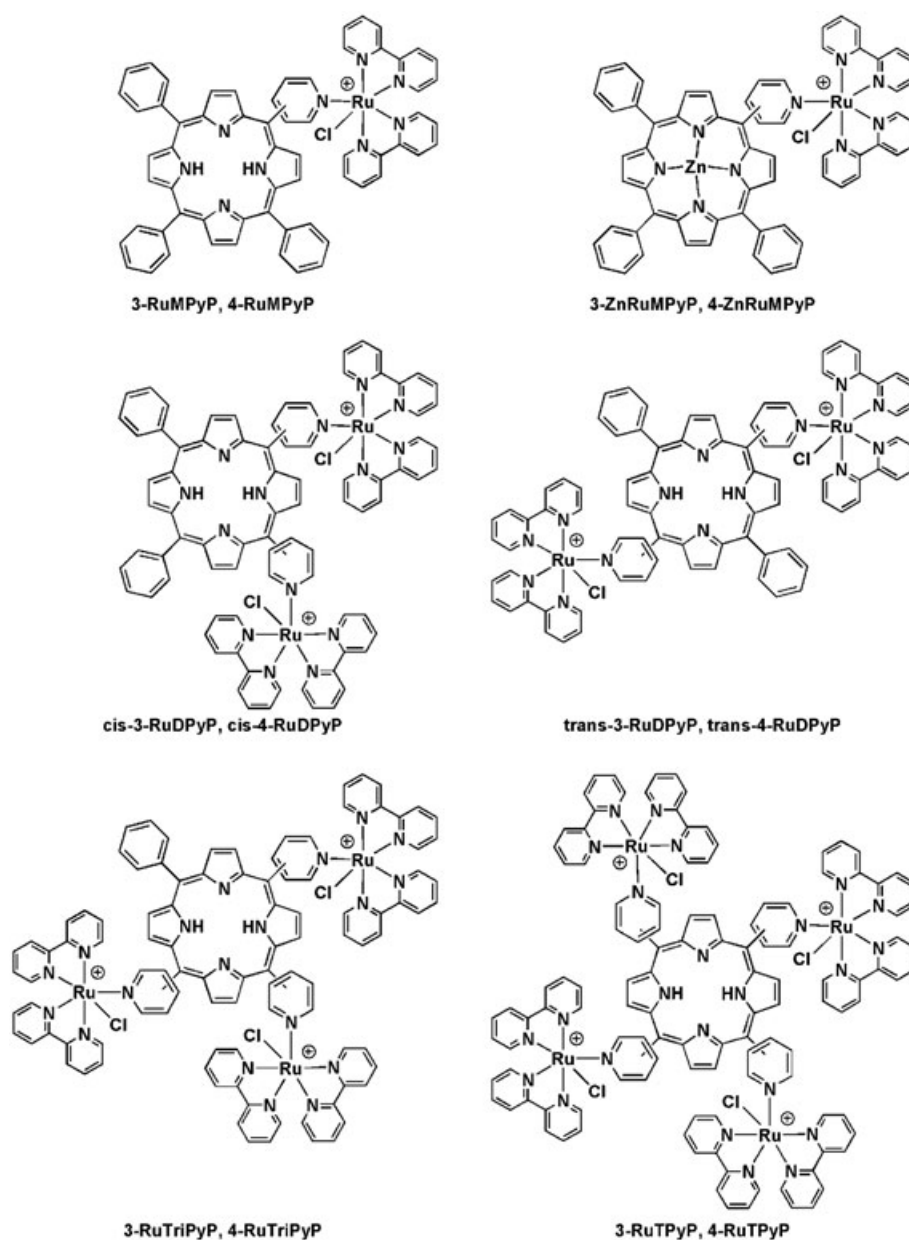
TWIM has been successfully used in a number of applications including structural studies and separation of isomers, such as drugs, anilines, oligosaccharides and peptides.^[18]

Herein we investigate the ability of ESI-TWIM-MS to resolve a series of pairs of cationic *para/meta* or *cis/trans* isomeric mono-, di-, tri- and tetra-ruthenated porphyrin complexes (Scheme 1).

EXPERIMENTAL

Synthetic procedures

Synthesis of the porphyrins^[8,19] yielded rather pure compounds and followed reported procedures as described in the Supporting Information.



Scheme 1. Wireframe structures of the N-ruthenated *meso*-pyridylporphyrin complexes.

Travelling wave ion mobility mass spectrometry experiments

ESI-TWIM-MS experiments were performed using a Synapt HDMS (high-definition mass spectrometer, Waters, Manchester, UK) mass spectrometer equipped with an ESI source. In this instrument, the TWIM cell entrance and exit apertures were reduced from 2 mm to 1 mm diameter to allow drift gas pressure to be efficiently increased to over 1 mbar without any substantial detrimental effect on MS performance. This instrument, described in detail elsewhere,^[17] has a hybrid quadrupole/ion mobility/orthogonal acceleration time-of-flight (oa-TOF) geometry. Instrument ESI source conditions were as follows: capillary voltage 3.0 kV, sample cone 30 V, extraction cone 3 V, source temperature 100 °C, desolvation temperature 100 °C, desolvation flow rate 400 mL min⁻¹ of N₂. For mobility separation, the TWIM cell was operated at a pressure of 1 mbar of nitrogen or carbon dioxide. When using nitrogen, wave velocity was set to 300 m/s and wave height was 13.6 V for multi-substituted porphyrins or 22.0 V for mono-substituted porphyrins. When carbon dioxide was used, wave parameters were 300 m/s and 27.0 V for multi-substituted porphyrins or 182 m/s and 30 V for mono-substituted porphyrins.

Theoretical calculations

Theoretical quantum chemical calculations were carried out at the semiempirical level using the HyperChemTM 8.0 program. Molecular structures were derived by full geometry optimization using a modified MM2 force field using a conjugate gradient of 10⁻³ kcal Å⁻¹ mol⁻¹ as convergence criterion. The SCF convergence tolerance was 10⁻⁵ kcal mol⁻¹ in all calculations.

RESULTS AND DISCUSSION

Spectroscopic characterization

Compounds **3-MPyP** and **4-MPyP** exhibit a typical porphyrin free-base electronic spectra in CH₂Cl₂ with a Soret and four Q bands at 418, 515, 548, 590 and 650 nm, and 420, 515, 550, 590 and 650 nm, respectively, for the *meta* and *para* isomers. The respective zinc complexes, **3-ZnMPyP** and **4-ZnMPyP**, exhibited the typical two Q banded spectral profile characteristic of metalloporphyrins. The **3-MRuPyP** and **4-MRuPyP** species exhibited bands at 293 nm, assigned to $\pi\text{-}\pi^*$ transitions localized at the bipyridyl ligands of the ruthenium(II) complex, and a broad band at 490 nm attributed to Ru^{II}(d π) \rightarrow bpy(p π^*) charge-transfer transitions, in addition to the typical porphyrin bands.

The ¹H-NMR spectra of the mono-ruthenated porphyrins were also consistent with the proposed structure showing the characteristic multiplets of bipyridyl protons around 8.00 to 10.00 ppm, as well as a multiplet around 9.00 ppm assigned to the β -pyrrole protons. The spectra of the free-base derivatives exhibited the typical inner ring protons (2H) signal around -2.80 ppm. The spectroscopic characterization of the multi-substituted porphyrin derivatives were consistent with those published elsewhere.^[5,8,10]

Travelling wave ion mobility

First, methanolic solutions of each porphyrin complex were separately subjected to ESI-TWIM-MS using N₂ as drift gas. Several wave voltages were tested but they showed little or no influence on isomer separations. Although voltage is known to influence peak width in IMS experiments,^[20] this effect was not observed for these species by TWIM. Figure 1(a) shows overlaid drift time plots for di(DPy), tri(TriPy) and tetra(TPy) ruthenated porphyrins, at the wave condition in which the largest number of species could fit the 0.0–9.0 ms window, whereas Figs. 1(b) (**3-RuMPyP**, **4-RuMPyP**) and 1(c) (**3-ZnRuMPyP** and **4-ZnRuMPyP**) show the overlaid drift time plots for the free-base and zinc(II) mono-ruthenated porphyrins (MPy). Note that the plots of Figs. 1(b) and 1(c) were acquired adjusting the wave height to speed up the singly charged MPy ions. Despite their larger volume and mass, each [Ru(bpy)₂Cl]⁺ substituent adds an extra charge to the porphyrin complex and the more highly charged complexes are subjected to higher acceleration by the TWIM electrical field. Therefore, TPy (+4) displays shorter drifts times, followed by Tri-Py (+3), DPy (+2) and MPy (+1). Figure 1 shows that all *meta* (**3-Ru**) and *para* isomers (**4-Ru**) were properly resolved by TWIM-MS, with the *meta* isomers (**3-Ru**) always displaying shorter drift times. This general trend suggests that **3-Ru** isomers are more compact than **4-Ru** isomers travelling therefore considerably faster through the drift gas. In contrast the two pairs of

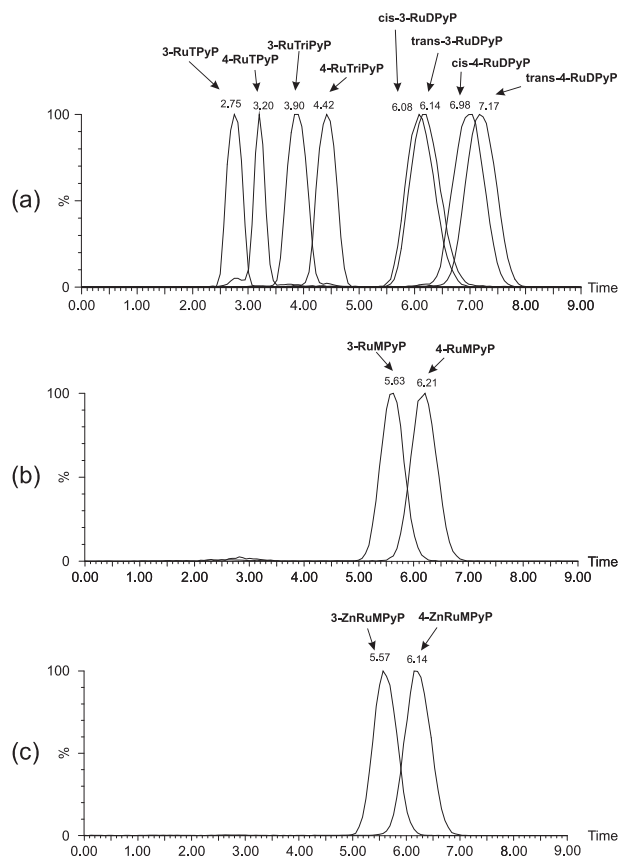


Figure 1. Overlaid drift time plots for (a) **3-RuTPyP**, **4-RuTPyP**, **3-RuTriPyP**, **4-RuTriPyP**, **cis-3-RuDPyP**, **cis-4-RuDPyP**, **trans-3-RuDPyP** and **trans-4-RuDPyP** (wave parameters: 300 m/s, 13.6 V), (b) **3-RuMPyP** and **4-RuMPyP** (wave parameters: 300 m/s, 22.0 V), and (c) **3-ZnRuMPyP** and **4-ZnRuMPyP** (wave parameters: 300 m/s, 22.0 V) using N₂ at 1 mbar of pressure as drift gas.

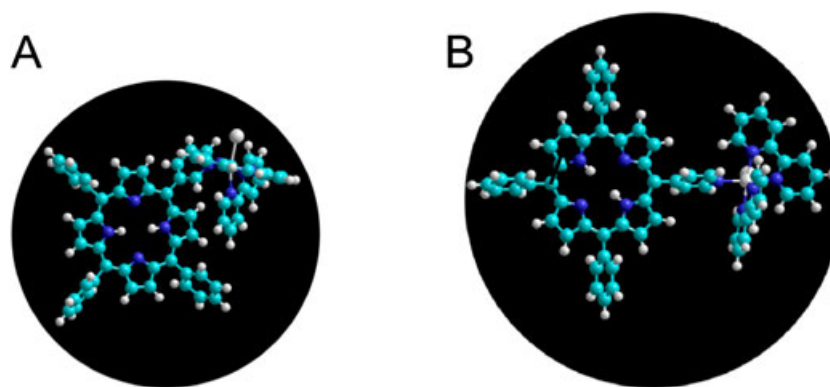


Figure 2. Optimized structures of the singly charged isomeric **3-MRuPyP** and **4-MRuPyP** (A, B) porphyrins using the MM-Plus method and convergence parameter of 1×10^{-4} kcal/Å.

cis/trans isomers displayed very close drift times, and could not be resolved by TWIM-MS in both N_2 and CO_2 (Figs. 1(a) and 3(a)).

The more compact structures of *meta* isomers were also indicated theoretically via structure optimization, as Fig. 2 shows for **3-RuMPyP** and **4-RuMPyP**. In fact, in the **3-Ru** species the ruthenium complex is more shifted towards the rotation volume of the porphyrin ring because it is bound at a shorter distance and forms a 120° instead of 180° angle with the porphyrin *meso* position.

The methanolic solutions of all porphyrin complexes were also subjected to ESI-TWIM-MS using CO_2 as drift gas (Fig. 3). Again wave height showed little or no influence on isomer separations and peak widths; however, a general trend was observed where the use of CO_2 as drift gas provided better resolution and narrower peaks as compared to N_2 . In order to better visualize how CO_2 affects the species separation and drift times in comparison to N_2 , Fig. 3 displays overlaid drift times acquired in CO_2 with wave parameters adjusted so that the faster ions (**3-RuTPyP** for Fig. 3(a) and **3-ZnRuMPyP** for Figs. 3(b) and 3(c)) displayed similar drift time as that obtained with N_2 (2.75 and 5.57 ms, respectively). As seen by comparing Figs. 1 and 3, the same order of elution and similar drift times and separation factors (α) were observed for all ions in CO_2 as compared to N_2 . But clearly CO_2 provides considerably narrower peaks, that is, improved resolving power (R_p) leading consequently to better peak-to-peak resolution (R_{p-p}).^a Table 1 compares, both in N_2 and CO_2 , the R_{p-p} , α and R_p values.

^aThe ability of a mobility cell to resolve two ions (see, for instance, Tabrizchi and Rouhollahnejad^[21]) can be measured by the peak-to-peak resolution, which is defined as:

$$R_{p-p} = \frac{2(t_{d2} - t_{d1})}{W_{b1} + W_{b2}}$$

in which t_{d_i} are the drift times of the two peaks whereas W_b is the peak width at the base line. R_{p-p} is a function of peak separation as measured by the separation factor (α) and peak width as measured by the resolving power (R_p), which are defined as:

$$\alpha = \frac{t_{d2}}{t_{d1}} \quad R_p = \frac{t_d}{W_{1/2}}$$

in which $W_{1/2}$ is the peak width at half of the maximum intensity. R_{p-p} relates to α and R_p as follows:

$$R_{p-p} = 0.589 R_p \frac{\alpha - 1}{\alpha}$$

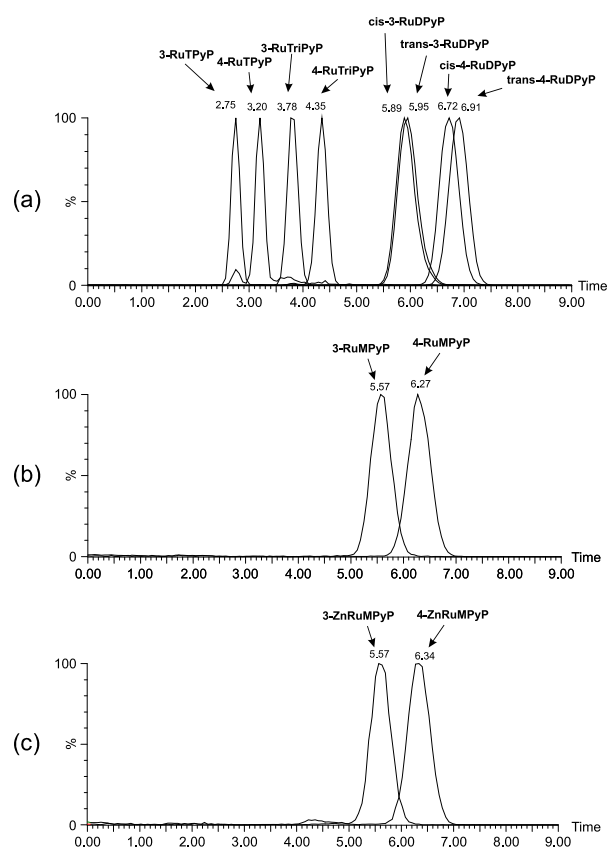
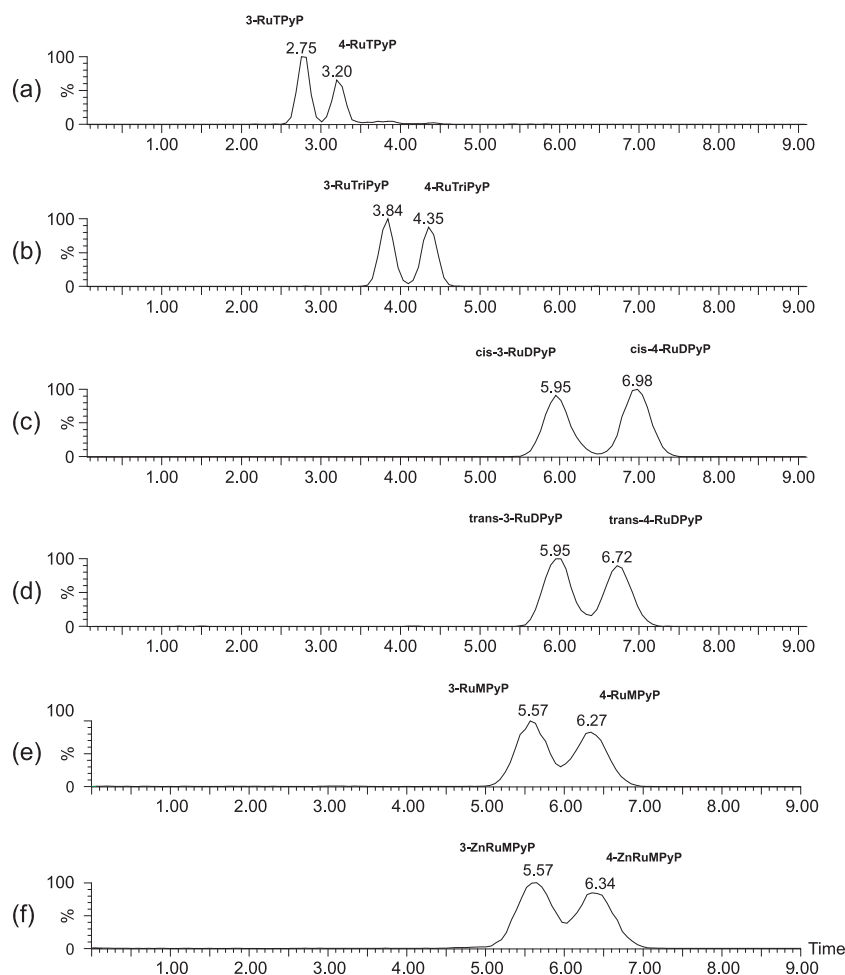


Figure 3. Overlaid drift time plots for (a) **3-RuTPyP**, **4-RuTPyP**, **3-RuTriPyP**, **4-RuTriPyP**, *cis*-**3-RuDPyP**, *cis*-**4-RuDPyP**, *trans*-**3-RuDPyP** and *trans*-**4-RuDPyP** (wave parameters: 300 m/s, 27.0 V), (b) **3-RuMPyP** and **4-RuMPyP** (wave parameters: 182 m/s, 30.0 V), and (c) **3-ZnRuMPyP** and **4-ZnRuMPyP** (wave parameters: 182 m/s, 30.0 V) using CO_2 at 1 mbar of pressure as drift gas.

For the MPy isomers, note that the R_{p-p} values for the *meta/para* pairs of isomers of the free-base and respective zinc(II) porphyrins were essentially the same in N_2 (0.42 vs. 0.43, Table 1), but the R_{p-p} values of the more rigid (and perhaps more polar) zinc(II) porphyrin isomers were considerably larger (0.56 vs. 0.63) in CO_2 .

Table 1. Peak-to-peak resolution (R_{p-p}), separation factor (α) calculated for each pair of isomers, and resolving power (R_p)^a

Isomeric pairs	N ₂			CO ₂		
	R_{p-p}	R_p	α	R_{p-p}	R_p	α
3-RuMPyP/4-RuMPyP	0.43	10.24	1.10	0.56	11.37	1.13
3-ZnRuMPyP/4-ZnRuMPyP	0.42	10.92	1.10	0.63	11.14	1.14
<i>cis</i> -3-RuDPyP/ <i>cis</i> -4-RuDPyP	0.56	9.85	1.14	0.74	15.50	1.14
<i>trans</i> -3-RuDPyP/ <i>trans</i> -4-RuDPyP	0.70	9.03	1.17	0.89	14.17	1.16
3-RuTriPyP/4-RuTriPyP	0.65	8.95	1.15	0.91	15.12	1.15
3-RuTPyP/4-RuTPyP	0.71	8.09	1.16	1.00	13.75	1.16
<i>cis</i> -3-RuDPyP/ <i>trans</i> -3-RuDPyP	0.02	9.85	1.00	0.05	15.50	1.01
<i>cis</i> -4-RuDPyP/ <i>trans</i> -4-RuDPyP	0.13	10.26	1.03	0.18	16.39	1.03

^a R_p was calculated for the faster isomer of the pair.**Figure 4.** Drift time plots for mixtures of (a) 3-RuTPyP and 4-RuTPyP, (b) 3-RuTriPyP and 4-RuTriPyP, (c) *cis*-3-RuDPyP and *cis*-4-RuDPyP, (d) *trans*-3-RuDPyP and *trans*-4-RuDPyP, (e) 3-RuMPyP and 4-RuMPyP, and (f) 3-ZnRuMPyP and 4-ZnRuMyP, using CO₂ at 1 mbar. (a)-(d) wave velocity 300 m/s and wave height 27 V; (e)-(f) wave velocity 182 m/s and wave height 30 V.

The results summarized in Table 1 show that CO₂ provides considerably better values of R_{p-p} than N₂ for all pairs of *meta/para* isomers. Note the extraordinary value of R_p in CO₂ (ca. 16) obtained for such a short (ca. 18 cm long) TWIM cell. R_{p-p} can be improved either by improving the separation factor ($\alpha = t_{d2}/t_{d1}$) or the resolving power R_p (peak width),

or both. Table 1 shows that the separation factor was quite similar for both N₂ and CO₂ ($\alpha \approx 1.1$) but considerably better values of R_p were obtained in CO₂. Therefore, the better value of R_{p-p} in CO₂ results mostly from peak narrowing, particularly for the multiply charged species (R_p for TPy for instance changed from ~ 8 in N₂ to ~ 14 in CO₂).

Mixtures were also tested (Fig. 4), and TWIM-MS was indeed able to separate all *meta/para* isomers in such mixtures. A reasonable value of R_{p-p} of 0.56 was observed for the MPy pair, whereas near baseline R_{p-p} was achieved for the other isomeric pairs in CO₂. The *cis/trans* isomers, however, could not be resolved, displaying very close drift times (Fig. 3(a)). It is clear therefore that *meta/para* isomerism in the Py substituent has a larger effect on either collision cross section or polarity of these cationic porphyrin complexes than the *cis/trans* isomerism (Scheme 1).

CONCLUSIONS

Isomeric *meta/para* and *cis/trans* pairs of cationic multi-ruthenated porphyrins with variable charge states (+1 up to +4) were prepared (Supporting Information), and the ability of TWIM-MS to perform the challenging task of resolving these isomers was tested using either N₂ or CO₂ as the drift gas. CO₂ has provided better R_{p-p} resolution for all pairs of *meta/para* isomers as compared to N₂. This improvement resulted essentially from substantial peak narrowing and hence better resolving power (R_p), whereas the separation factor was essentially the same for both gases. The more compact *meta* isomers were found to display shorter drift times than the *para* isomers, and R_{p-p} was substantially increased for the multiply charged species: MPy (+1) < DPy (+2), TriPy (+3), TPy (+4). The *cis/trans* isomers investigated displayed, however, very close drift times both in CO₂ and N₂ and TWIM-MS was unable to properly resolve this class of porphyrin isomers. These results should guide further attempts to resolve other mixtures of isomeric porphyrins and related species by TWIM-MS.

SUPPORTING INFORMATION

Additional supporting information may be found in the online version of this article.

Acknowledgements

We thank FAPESP, CNPq, CAPES and INOMAT for financial support.

REFERENCES

- [1] K.M. Kadish, K.M. Smith, R. Guilard. *The Porphyrin Handbook*, vols. 1–20. Academic Press, San Diego, 2000–2003.
- [2] (a) M. Jurowa, A.E. Schuckman, J.D. Batteas, C.M. Drain. *Coord. Chem. Rev.* **2010**, 19/20, 2297; (b) J. Setsune. *J. Porph. Phthalocyan.* **2004**, 8, 93.
- [3] (a) H.E. Toma, K. Araki, in *Progress In Inorganic Chemistry*, vol. 56, (Ed: K.D. Karlin), John Wiley, New York, **2009**, pp. 379–485; (b) K. Araki, H.E. Toma, in *N4-Macrocyclic Metal Complexes*, (Eds: J. Zagal; F. Bedioui and J.D. Dodelet), Springer, New York, **2006**, pp. 255–314.
- [4] M.E. Ojaimi, B. Habermeyer, C.P. Gros, J.-M. Barbe. *J. Porph. Phthalocyan.* **2010**, 14, 469.
- [5] K. Araki, C.A. Silva, H.E. Toma, L.H. Catalani, M.H.G. Medeiros, P.D. Mascio. *J. Inorg. Biochem.* **2000**, 78, 269.
- [6] D.R. McMillin, A.H. Shelton, A. Bejune, Ph. E. Fanwick, R. K. Wall. *Coord. Chem. Rev.* **2005**, 249, 1454.
- [7] K. Zupán, M. Egyeki, K. Tóth, A. Fekete, L. Herényi, K. Módos, G. Csík. *J. Photochem. Photobiol. B* **2008**, 90, 105.
- [8] (a) F.M. Engelmann, H. Winnischofer, K. Araki, H.E. Toma. *J. Porphyr. Phthalocyan.* **2002**, 6, 33; (b) F.M. Engelmann, I. Mayer, D.S. Gabrielli, H.E. Toma, A.J. Kowaltowski, K. Araki, M.S. Baptista. *J. Bioenerg. Biomembr.* **2007**, 39, 175.
- [9] J.B. Fenn, M. Mann, C.K. Meng, S.F. Wong, C.M. Whitehouse. *Science* **1989**, 246, 64.
- [10] (a) D.M. Tomazela, F.C. Gozzo, I. Mayer, F.M. Engelmann, K. Araki, H.E. Toma, M.N. Eberlin. *J. Mass Spectrom.* **2004**, 39, 1161; (b) I. Mayer, M.N. Eberlin, D.M. Tomazela, H.E. Toma, K. Araki. *J. Braz. Chem. Soc.* **2005**, 16, 418; (c) I. Mayer, A.L.B. Formiga, F.M. Engelmann, H. Winnischofer, P.V. Oliveira, D.M. Tomazela, M.N. Eberlin, H.E. Toma, K. Araki. *Inorg. Chim. Acta* **2005**, 358, 2629; (d) S.H. Toma, A.D.P. Alexiou, H.E. Toma, M.N. Eberlin, K. Araki. *J. Mass Spectrom.* **2009**, 44, 361.
- [11] (a) W.A. Tao, F.C. Gozzo, R.G. Cooks. *Anal. Chem.* **2001**, 73, 1692; (b) L. Wu, E.C. Meurer, B. Young, P. Yang, M.N. Eberlin, R.G. Cooks. *Int. J. Mass Spectrom.* **2004**, 231, 103.
- [12] (a) J. Stach, J.I. Baumbach. *Int. J. Ion Mobility Spectrom.* **2002**, 5, 1; (b) A.B. Kanu, P. Dwivedi, M. Tam, L. Matz, H.H. Hill Jr. *J. Mass Spectrom.* **2008**, 43, 1.
- [13] (a) R.G. Ewing, D.A. Atkinson, G.A. Eiceman, G.J. Ewing. *Talanta* **2001**, 54, 515; (b) D.C. Collins, M.L. Lee. *Anal. Bioanal. Chem.* **2002**, 372, 66.
- [14] (a) G. Von Helden, T. Wyttenbach, M.T. Bowers. *Science* **1995**, 267, 1483; (b) D.E. Clemmer, R.R. Hudgins, M.F. Jarrold. *J. Am. Chem. Soc.* **1995**, 117, 10141; (c) C.S. Hoaglund-Hyzer, A.E. Counterman, D.E. Clemmer. *Chem. Rev.* **1999**, 99, 3037.
- [15] (a) P. Dwivedi, B. Bendiak, B.H. Clowers, H.H. Hill. *J. Am. Soc. Mass Spectrom.* **2007**, 18, 1163; (b) S. Trimpin, D.E. Clemmer. *Anal. Chem.* **2008**, 80, 9073; (c) F.A. Fernandez-Lima, C. Becker, A.M. McKenna, R.P. Rodgers, A.G. Marshall, D.H. Russell. *Anal. Chem.* **2009**, 81, 9941.
- [16] P. Dwivedi, C. Wu, L.M. Matz, B.H. Clowers, W.F. Siems, H.H. Hill Jr. *Anal. Chem.*, **2006**, 78, 8200.
- [17] (a) K. Giles, S.D. Pringle, K.R. Worthington, D. Little, J.L. Wildgoose, R.H. Bateman. *Rapid Commun. Mass Spectrom.* **2004**, 18, 2401; (b) S.D. Pringle, K. Giles, J.L. Wildgoose, J.P. Williams, S.E. Slade, K. Thalassinos, R.H. Bateman, M.T. Bowers, J.J. Scrivens. *Int. J. Mass Spectrom.* **2007**, 261, 1; (c) A.A. Shvartsburg, R.D. Smith. *Anal. Chem.* **2008**, 80, 9689; (d) D.P. Smith, T.W. Knapman, I. Campuzano, R.W. Malham, J.T. Berryman, S.E. Radford, A.E. Ashcroft. *Eur. J. Mass Spectrom.* **2009**, 15, 113; (e) B.T. Ruotolo, K. Giles, I. Campuzano, A.M. Sandercock, R.H. Bateman, C.V. Robinson. **2005**, 310, 1658.
- [18] (a) M. Benassi, Y.E. Corilo, D. Uria, R. Augusti, M.N. Eberlin. *J. Am. Soc. Mass Spectrom.* **2009**, 20, 269; (b) H.I. Kim, H. Kim, E.S. Pang, E.K. Ryu, L.W. Beegle, J.A. Loo, W.A. Goddard, I. Kanik. *Anal. Chem.* **2009**, 81, 8289; (c) G.R. Hilton, K. Thalassinos, M. Grabenauer, N. Sanghera, S.E. Slade, T. Wyttenbach, P.J. Rosinson, T.J.T. Pinheiro, M.T. Bowers, J. H. Scrivens. *J. Am. Soc. Mass Spectrom.* **2010**, 21, 845; (d) L. F. Santos, A.H. Iglesias, E.J. Pilau, A.F. Gomes, F.C. Gozzo. *J. Am. Soc. Mass Spectrom.* **2010**, 12, 2062; (e) P.M. Lalli, Y.E. Corilo, G.F. Sa, R.J. Daroda, V. Souza, G.H.M.F. Souza, I. Campuzano, G. Ebeling, J. Dupont, M.N. Eberlin. *Chem. Phys. Chem.* **2011**, 12, 1444; (f) W. Romao, P.M. Lalli, M.F. Franco, G. Sanvido, N.V. Schwab, R. Lanaro, J.L. Costa, B.D. Sabino, M.I.M.S. Bueno, G.F. Sa, R.J. Daroda, V. Souza, M.N. Eberlin. *Anal. Bioanal. Chem.* **2011**, 400, 3053; (g) Y.-T. Chan, X. Li, J. Yu, G.A. Carri, C.N. Moorefield, G.R. Newkome, C. Wesdemiotis. *J. Am. Chem. Soc.* **2011**, 133, 11967.
- [19] E.B. Fleisher, A.M. Shachter. *Inorg. Chim.* **1991**, 30, 3763.
- [20] G.R. Absury, H.H. Hill. *Anal. Chem.* **2000**, 72, 580.
- [21] M. Tabrizchi, F. Rouholahnejad. *Talanta* **2006**, 69, 87.